Chemical influences on adsorption-mediated self-propelled drop movement

Seok-Won Lee,* Daniel Y. Kwok,† and Paul E. Laibinis‡
Department of Chemical Engineering, Massachusetts Institute of Technology, Cambridge, Massachusetts 02139
(Received 15 November 2001; published 2 May 2002)

We report studies of reactive wetting employing droplets of a nonpolar liquid (decahydronaphthalene) on chemically patterned surfaces. The drops contain an *n* alkylamine that adsorbs onto surfaces exposing carboxylic acid groups and produces surfaces exposing methyl groups. The change in surface energy that occurs concurrent with the formation of an oriented monomolecular film of alkylamine during this process is sufficient to produce a self-propelled movement of decahydronaphthalene drops on the surface. We employed patterning to direct the movement of the drops on the surface, thereby allowing measurements of the relationships between the macroscopic fluidic behavior of the droplets and microscopic adsorption events. Specifically, we examined the effects of the unbalanced surface-tension force and the influences of adsorbate concentration on drop movement. In this latter case, both kinetic and thermodynamic arguments can be applied to describe the system. We compared the predictions from these two approaches by analyzing data from the present system and those reported by F. Domingues Dos Santos and T. Ondarcuhu [Phys. Rev. Lett. **75**(16), 2972 (1975)] that exhibited opposite trends in behavior. The present analysis provides insight into the influence of chemical reaction kinetics on adsorption-mediated drop movement (i.e., reactive wetting).

DOI: 10.1103/PhysRevE.65.051602 PACS number(s): 68.08.Bc, 68.43.Mn, 81.16.Dn

I. INTRODUCTION

Solid-liquid interactions play an important role in the design and operation of numerous processes. Current interests in microfluidics, microdroplet handling, microarray generation, and integrated microsystems share common requirements of handling and manipulating fluidic behavior in cases dominated by surface effects [1–9]. The behavior of these systems is influenced by a variety of microscopic factors and cannot be easily described. Capillary forces and other surface effects are sufficient to alter fluidic behavior due to the proportionately large areas of solid-liquid contact on these affected small volumes.

A number of recent theoretical and experimental studies [10–20] have shown that drop motion can be initiated and self-propelled by a surface energy gradient on a substrate. Such gradients can be generated either passively using surfaces with spatial variations in free energy [17,19] or actively using surfactantlike agents that adsorb onto the contacted surface and induce localized dewetting events [10,16,18,20]. The former approach has been effectively developed by Chaudhury and Whitesides using oxide surfaces that have been modified to expose a monotonically decreasing coverage of immobilized alkyl chains along the direction that propels drop movement [17,19]. Examples of the latter include the self-propelled movement on glass surfaces of hydrocarbon drops containing fatty acids, or alkyltrichlorosilanes [10,16]. In these experiments, the adsorbate modifies the glass surface and decreases the wettability of the substrate. The change in wettability effected by contact with the reactive drop results in its self-propelled movement on the glass surface. Domingues Dos Santos and Ondarcuhu have studied the movement of octane and dodecane drops containing 1,1,2,2-tetrahydroperfluorodecyltrichlorosilane $[CF_3(CF_2)_7(CH_2)_2SiCl_3]$ on glass and examined the effects of silane concentration and drop length on drop movement [10]. These different approaches provide a collection of methods for moving liquids within microscale systems and avoid the need for mechanical parts, pumps, or external forces for driving liquid flow.

In this paper, we examine the effects of adsorbate chain length, concentration, and drop length on reactive wetting on chemically patterned surfaces. We employed decahydronaphthalene droplets that contain various amounts of an *n*-alkylamine to reactively wet and move about surfaces that expose a dense packing of carboxylic acid functionalities. The amine compounds adsorb onto this surface and produce one with a lower energy that exposes methyl groups, thereby causing a local surface energy gradient that is sufficient to induce a self-propelled movement of the contacting droplets on the surface. We employ patterning methods (microcontact printing, [21]) to confine the direction of drop movement on these surfaces, thereby allowing direct measurement of fluidic movement and velocity. This ability allowed examination of the relationships between macroscopic droplet behavior and microscopic adsorption events. Specifically, we examined the effects of the force due to the unbalanced surface tension and of drop composition (adsorbate concentration and drop size) on the drop velocity, and analyzed these results using both thermodynamic and kinetic considerations. The former effect was examined by varying the molecular structure of the adsorbate as a means to produce functionalized surfaces with different wetting properties. These studies established fundamental relationships [20] that are expanded

*Present address: Biosite, Inc., San Diego, CA; electronic address: SEOKWON@ALUM.MIT.EDU

†Present address: Department of Mechanical Engineering, University of Alberta, Edmonton, Alberta, Canada T6G 2G8; electronic address: DANIEL.Y.KWOK@UALBERTA.CA

‡Corresponding author. FAX: (617) 258-5042; electronic address: PEL@MIT.EDU

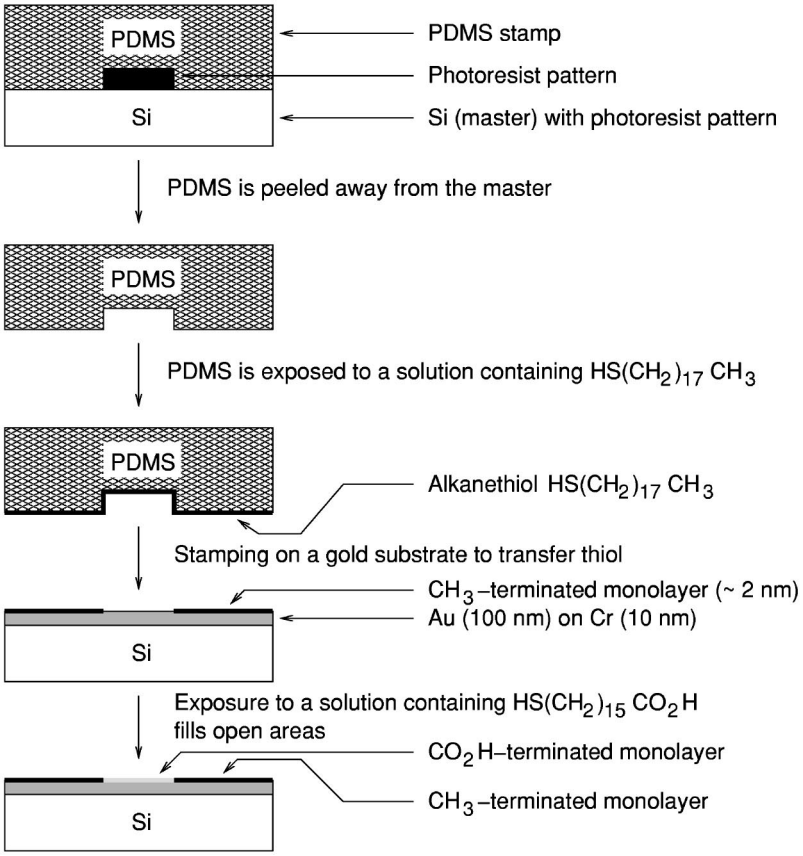

FIG. 1. Schematic overview of the process for preparing the patterned elastomeric stamp and its use in the generation of patterned areas exposing CH_3 and CO_2H surfaces. These different regions are illustrated as black and gray coated areas, respectively, on the Si/Cr/Au substrate.

in their analysis here by considering the influences of reaction kinetics.

II. MATERIAL AND METHODS

A. Materials

Silicon wafers were test grade and obtained from Silicon Sense (Nashua, NH). Gold shot (99.99%) and chromium-coated filaments were obtained from Americana Precious Metals (East Rutherford, NJ) and R.D. Mathis Co. (Long Beach, CA), respectively. Stamps for generating patterned surfaces by microcontact printing [21] were made of poly(dimethylsiloxane) (PDMS) as sold by Dow-Corning (Midland, MI) as SYLGARD Silicon Elastomer-184. Decahydronaphthalene (anhydrous, mixture of *cis* and *trans*) and *n*-alkylamines [C_nNH_2, $n=6$, 8, 10, 14, and 18] were obtained from Aldrich (Milwaukee, WI) and used as received. Ethanol (190 proof) was obtained from Pharmco (Weston, MO). Octadecanethiol [$CH_3(CH_2)_{17}SH$] was obtained from Aldrich and purified by recrystallization. 16-Mercaptohexadecanoic acid [$HS(CH_2)_{15}CO_2H$] was synthesized according to literature procedures [22].

B. Substrates preparation

Supported gold films were prepared by sequentially evaporating chromium ($\sim$10 nm) and gold ($\sim$100 nm) onto silicon wafers in a diffusion-pumped vacuum chamber at $\sim 10^{-6}$ torr. The chamber was backfilled with air and the substrates were used within 48 h of preparation.

C. Formation of patterned surfaces

Figure 1 provides a schematic overview of the microcontact printing process and it is used to generate patterned surfaces for directing drop movement. In the first step, masters for fabrication of the elastomeric stamps used for microcontact printing a self-assembled monolayer film pattern on the gold surface were prepared using conventional photolithography methods as described elsewhere [21]. The masters, consisting of a developed photoresist film with the desired features (negative 2×60 mm^2 rectangular tracks), were placed in a plastic or glass petri dish. A 10:1 ratio (w:w) mixture of SYLGARD silicone elastomer 184 and its curing agent was poured over the master to a thickness of 5–10 mm. The mixture was allowed to cure either at room temperature overnight or at 65 °C for 1–3 h. Sections of the polymer were cut with a razor blade and then peeled from the master, producing a negative copy of the master on the PDMS surface. The peeled sections were washed several times with ethanol and dried with a stream of N_2 before use. The generated PDMS stamp was ''inked'' by directly pouring a 5 mM ethanolic solution of octadecanethiol on the patterned PDMS stamp. After inking, the stamp was placed gently on a gold substrate and removed after 3–5 min to produce a pattern of octadecanethiol-coated areas and bare gold regions. The remaining unfunctionalized surface (2×60 mm^2 tracks) was derivatized by immersion of the slide into a 5 mM ethanolic solution of 16-mercaptohexadecanoic acid [$HS(CH_2)_{15}CO_2H$] for $\sim$5 min. This step completed formation of a patterned surface consisting of a series of 2

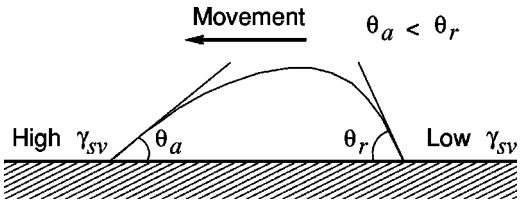

FIG. 2. Schematic illustration of a moving droplet under the influence of a surface energy gradient. A requirement is that the advancing contact angle (θ_a) on the forward-moving side of the drop be lower than the receding contact angle (θ_r) on the backside.

$\times 60$ mm^2 tracks that exposed a CO_2H surface, each surrounded by areas expressing a low-energy CH_3-terminated surface. The samples were rinsed sequentially with ethanol and deionized water, and blown dry with N_2 before use.

D. Moving drop velocity measurements

Moving drop experiments were performed in the open laboratory under atmospheric conditions. Drops (~ 1 μL) were deposited at one end of a CO_2H exposing track using a microliter syringe and monitored. These drops spontaneously moved unassisted in a straight path to the opposite end of the track. Images of the moving drops (in top view) were taken using a charge-coupled device (CCD) camera (60 frames/s) equipped with a microscopic lens, synchronized strobe illumination, and super video home system (SVHS) recorder. These temporal images were analyzed to determine steady-state drop velocities.

III. RESULTS AND DISCUSSION

A. Background on experimental approach

Our generation of self-propelled drop movement relies on the conversion of a high-energy surface to a low-energy surface that induces a change in wettability sufficient to provide the energetic driving force for drop movement (see Fig. 2). For our base surface, the adsorption of a mercapto-alkanoic acid [$HS(CH_2)_nCO_2H$] onto gold generates a densely packed supported monolayer film that exposes carboxylic acid groups at its surface. These high-energy surfaces are wet by most liquids including water [26]. Previously, we reported [20] that these surfaces could be modified by contact with a nonpolar solution containing an *n*-alkylamine. In this process, the amino group undergoes an acid-base reaction with the surface carboxylic acid group and generates a noncovalently attached oriented monolayer of the alkylamine at its surface. The resulting bilayer exposes the methyl groups (CH_3) of the alkylamine at its surface, as evidenced by its wetting properties by water and various hydrocarbon liquids [20]. Exposure of the bilayer to a polar solvent removes the amine layer and regenerates the high-energy carboxylic acid surface. The resulting surfaces are less wettable (i.e., exhibit higher values of θ_a and θ_r) when alkylamines of longer chain lengths or solutions of higher amine concentrations are employed [20].

The adsorption process to generate the amine adlayer can effect a self-propelled drop movement on the carboxylic acid surface when the applied droplet contains sufficient amine to effect adsorption and the liquid has a sufficiently high surface tension ($\gamma_{lv} > 30$ mJ/m^2) so to not wet the generated methyl surface. Under these conditions (for example, a 1 mM drop of dodecyl amine in benzene), a drop applied to an unpatterned carboxylic acid surface will spontaneously move about the surface in a meandering self-propel and self-avoiding path as it converts its contacted areas to lower-energy CH_3 surface regions.

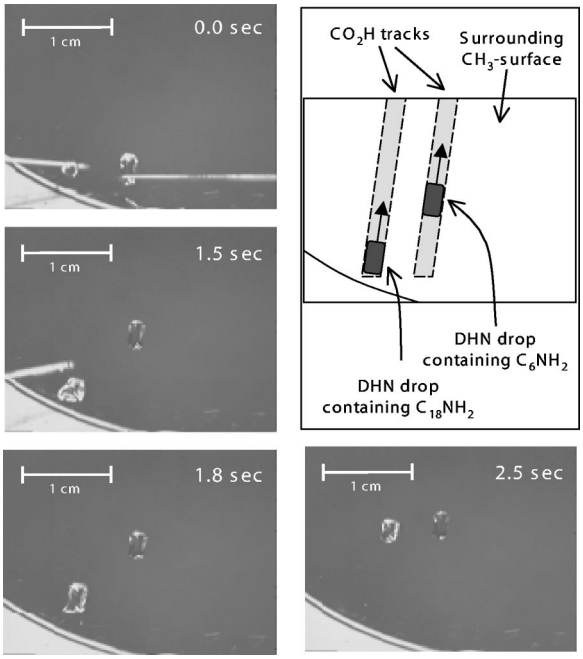

FIG. 3. Series of images for two *n*-alkylamine-containing DHN drops on patterned CO_2H/CH_3 surfaces. Upper right: schematic illustration of the patterned surface comprising 2×60 mm^2 CO_2H tracks surrounded by CH_3-terminated domains that restricted the drop movement. Upper left and counterclockwise: Images following the movement of C_6NH_2- and $C_{18}NH_2$-containing DHN drops deposited. Drops were deposited sequentially 1.5 s apart at the ends of different tracks, with the images showing their spontaneous movement and the faster velocity of the $C_{18}NH_2$-containing DHN drop (right track).

To control the process, we employed microcontact printing [21] to generate patterned surfaces that presented definable paths—2×60 mm^2 rectangular tracks—for drop movement. The patterned surfaces exposed tracks of a CO_2H-terminated self-assembled monolayer (SAM) and a boundary of a CH_3-terminated SAM (see Fig. 3 inset). This latter surface was not wet by the droplet and exposed the same chemical functionality as produced upon adsorption of the *n*-alkylamine onto the CO_2H surfaces. A droplet of decahydro-naphthalene (DHN), a nonpolar liquid with a surface tension of 41 mJ/m^2, containing an *n*-alkylamine placed at one end of a track, moved on the surface along the path defined by the microcontact printing process (Fig. 3). The movement of the drops along linear paths eased determination of drop velocities and allowed examination of factors that influence the fluid's behavior.

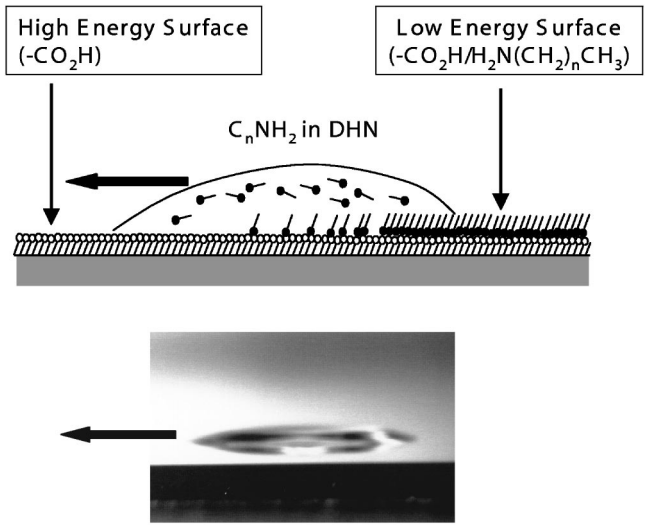

FIG. 4. Schematic illustration of the surface energy change induced by adsorption of an *n*-alkylamine onto a CO_2H surface. The lower image shows the side view of a moving drop (including its reflection on the gold substrate) and its apparent asymmetric shape (i.e., $\theta_a < \theta_r$).

B. Effect of adsorbate chain length

Figure 3 shows a sequence of images for two DHN droplets, each applied to the end of one of two parallel CO_2H-exposing tracks in sequence, that contained 1 mM solutions of either C_6NH_2 or $C_{18}NH_2$. The images show that the movements of the drops are confined by the microcontact printed CH_3 surfaces. These drops were deposited sequentially 1.5 s apart at the ends of different tracks, with images showing their spontaneous movement. An analysis of images from such experiments found that the DHN drop containing the $C_{18}NH_2$ moved faster (~ 0.8 cm/s) than that containing the C_6NH_2 (~ 0.5 cm/s). Studies of DHN drops containing *n*-alkylamines of intermediate chain lengths ($n=8$, 10, and 14) exhibited velocities that showed a general increase with chain length. For all amines, these molecules adsorb onto the CO_2H surface and form oriented monolayer films on the contacted areas that expose the CH_3 group at the monolayer/air (liquid) interface. The effected change in surface functionality and corresponding change in surface energy provides the energetic driving force for drop movement. The longer-chained *n*-alkylamines form a thicker molecular layer on the CO_2H surface to produce coatings that better mask the presence of the underlying polar functionalities and yield surfaces that are less wet by DHN [23].

In these experiments, we expect the dominant force responsible for drop movement to be the unbalanced surface tension force F_Y that results from the difference in wettability or surface energy between the front and the back sides of the drop (see Figs. 2 and 4)

$$F_Y = \gamma_{lv}(\cos\theta_a - \cos\theta_r) \tag{1}$$

where γ_{lv} is the surface tension of the liquid, and θ_a and θ_r are the advancing and receding contact angles of DHN on the native CO_2H surface and on the amine-derivatized surface, respectively. In these experiments, DHN wets the CO_2H surface (i.e., $\theta_a \simeq 0°$) and recedes from the amine-derivatized surface with a nonzero contact angle (i.e., $\theta_r > 0°$). Thus, Eq. (1) predicts that the unbalanced surface force imposed on drops applied to a bare CO_2H surface depends directly on the receding contact angle on the resulting amine-derivatized surface.

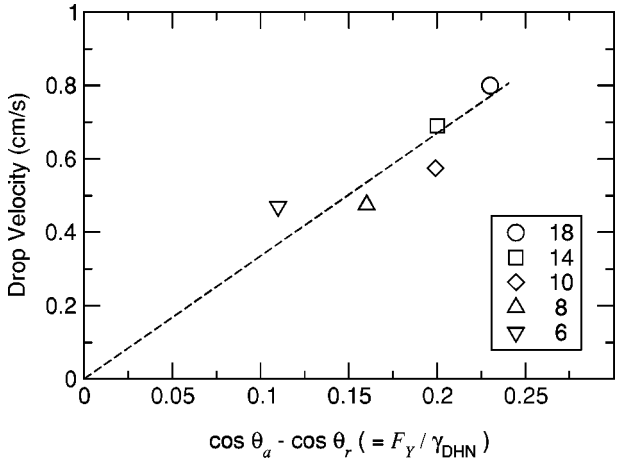

FIG. 5. The velocity of various *n*-alkylamine (C_nNH_2)-containing DHN drops on CO_2H surfaces versus the change in wetting induced by adsorption of the amine ($\cos\theta_a - \cos\theta_r$). The dashed line is a fit of Eq. (2) to the data.

Figure 5 plots the steady-state velocities of DHN drops containing different *n*-alkylamines as a function of the value of $\cos\theta_a - \cos\theta_r$. The data exhibit a linear relationship between the applied surface force and the measured steady-state velocity. Under these conditions, the forces on the drop must balance, and the viscous drag force must be equal to the unbalanced surface force [20] on the moving drop [Eq. (1)]:

$$W\gamma_{lv}(\cos\theta_a - \cos\theta_r) = \frac{A\mu V}{h}, \tag{2}$$

where μ is the viscosity of the liquid; W is the length of contact lines at the front and rear of the drop and is roughly the width of track; A is the contact area between the drop and substrate; μ is the viscosity of the liquid; V is the drop velocity; and h is a characteristic length that approximates the mean height of the drop as averaged over the drop/substrate contact area with respect to the local drag force. From Fig. 5, we obtain a value for the proportionality constant, $Wh\gamma_{lv}/A\mu$, of $\simeq 3.6$ cm/s and a value for h of ~ 1.0 μm, suggesting that the viscous drag on the moving drop is localized primarily near the liquid/solid interface [20]. The assumed values for γ_{lv} and μ are 41 mJ/m^2 and 1×10^{-3} Ns/m^2, respectively. The suggestion from Fig. 5 and Eq. (2) is that changes to the wetting properties of the converted surface induce direct and correlated changes to the velocity of self-propelled drops on these surfaces. We have reported this observation previously [20] and we include it here as Eq. (2) and the determined parameters are used in our subsequent analyses for the kinetic factors that influence drop movement.

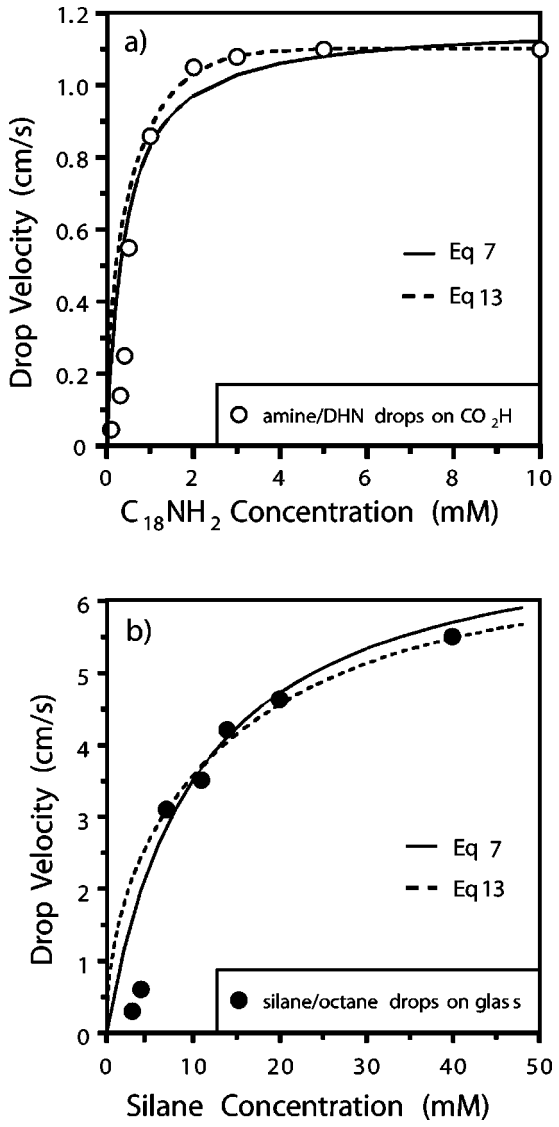

FIG. 6. Effect of adsorbate concentration on the velocity of self-propelled moving drops. (a) Data for the movement of DHN drops induced by the adsorption of $C_{18}NH_2$ onto CO_2H surfaces. (b) Data taken from Ref. [10] for the movement of *n*-octane drops induced by the adsorption of $CF_3(CF_2)_7(CH_2)_2SiCl_3$ onto a glass surface. The fits in both panels are to equations generated by considering equilibrium and kinetic influences [Eqs. (7) and (13), respectively] (see text). Table I summarizes the relevant fitting parameters for the two data sets.

C. Effect of Adsorbate Concentration on Drop Velocity

1. Propulsion of DHN drops on CO_2H surfaces by adsorption of $C_{18}NH_2$

A factor that will influence the effected change in surface energy upon adsorption of an *n*-alkylamine onto a CO_2H surface is the resulting surface coverage of the adsorbate. Higher coverages of the alkylamine would be expected to generate lower-energy surfaces and thus produce greater surface forces for (faster) drop movement. We observed that increases in the amount of an *n*-alkylamine present in the DHN drop effected faster drop movements. Figure 6(a) plots the effect of $C_{18}H_{37}NH_2$ concentration on the velocities of ~ 1 μL DHN drops applied to patterned CO_2H surfaces. The data show a relatively linear increase for concentrations less than ~ 0.5 mM of this amine and an asymptotic value for concentrations greater than ~ 2 mM. We hypothesize that the differences in drop velocities result from variations in the surface coverage of the alkylamine, as effected either by equilibrium or kinetic factors on the adsorption process, both of which would be affected by adsorbate concentration. We consider both regimes below separately after development of expressions to relate drop velocities and adsorbate surface compositions.

For drop movement experiments performed on CO_2H surfaces, Eq. (2) can be rewritten as

$$V=\kappa(\cos\theta_a-\cos\theta_r)\simeq\kappa(1-\cos\theta_r), \tag{3}$$

where $\kappa=Wh\gamma_{lv}/A\mu$ and $\theta_a=0°$. In Eq. (3), θ_r will depend on the composition of the derivatized surface. To describe this relationship, we use the Cassie equation [24]

$$\cos\theta_r=\sum_i x_i\cos\theta_{i,r}=x\cos\theta_{100,r}+(1-x)\cos\theta_{0,r}$$

$$\simeq 1-(1-\cos\theta_{100,r})x, \tag{4}$$

where x is the fractional composition of adsorbed amines, and $\theta_{100,r}$ and $\theta_{0,r}$ are the receding contact angles for complete adlayers (i.e., 100%) and bare CO_2H surfaces (i.e., 0%), respectively. As DHN wets a pure CO_2H surface, $\theta_{0,r}\simeq 0°$. Equation (4) provides a description of the incremental influence of adsorbed amine on the wetting properties of the modified surfaces. Substitution of Eqs. (4) into (3) yields

$$V=\kappa(1-\cos\theta_{100,r})x \tag{5}$$

for relating drop velocities on pure CO_2H surfaces to the adsorbate coverage x and the wetting properties of a complete amine adlayer.

2. Equilibrium analysis

The adsorption of the amine onto the CO_2H surface proceeds by a noncovalent association between the amine adlayer and the underlying CO_2H surface. The adsorption process is not permanent as the amine layer can be removed by rinsing the assembly with a polar solvent. Further, the amine adlayer can be replaced by exposure to a solution containing a different amine [20]. Because of these associative and dissociative factors, the coverage of adsorbed amine on the CO_2H surface is likely to be affected by equilibrium influences. Within this framework, we relate the fractional surface coverage of the amine x in Eq. (5) to its solution concentration in the DHN drop through the Langmuir adsorption equation [Eq. (6)]

$$x=\frac{Kc}{1+Kc}, \tag{6}$$

where K is the adsorption coefficient and c is the concentration of amine in the contacting DHN drop. In our experi-

TABLE I. Summary of the determined adsorption constant K and rate constant k from Eqs. (7) and (13), respectively.

Reactive wetting system Liquid/adsorbate/surface	K (L/mol)	k (L/mol-s)
DHN/$C_{18}H_{37}NH_2$/CO_2H	2800	3500
n-octane/$CF_3(CF_2)_7(CH_2)_2SiCl_3$/glass[a]	95	1100 [a]

[a]Reference [10].

ments, the amount of adsorbed amine is small compared to that in solution, and we consider c to be unchanged through the adsorption process. We selected a Langmuir adsorption isotherm for describing the amine adsorption process as this approach assumes that the adsorption is limited to a monolayer coverage, there are of specific sites for adsorption, and the dominant interactions for adsorption are between the surface sites and the adsorbates. For the present system, the amines adsorb stoichiometrically onto the CO_2H sites, they form a monolayer on the CO_2H surface, and the acid-base interaction between the amine and CO_2H groups is the primary energetic contributor that directs assembly. Further, the Langmuir isotherm provides one of the simplest descriptions of adsorption and avoids the introduction of additional parameters.

By combining Eqs. (5) and (6), we obtain an equilibrium-based expression for describing the dependence of drop velocity on concentration as

$$V=\kappa(1-\cos\theta_{100,r})\frac{Kc}{1+Kc}. \tag{7}$$

A useful limit is at high amine concentrations, where Eq. (7) reaches a maximum drop velocity $V_{c\to\infty}$ of

$$V_{c\to\infty}=\kappa(1-\cos\theta_{100,r})\lim_{c\to\infty}\frac{Kc}{1+Kc}=\kappa(1-\cos\theta_{100,r}). \tag{8}$$

Using the value of $\kappa=3.6$ cm/s obtained from the data in Fig. 5 and an experimental value of $\theta_{100,r}\simeq 47°$ on a complete $C_{18}NH_2$ adlayer, Eq. (8) yields a maximum drop velocity of 1.15 cm/s. Using these values for Eq. (7), the data in Figure 6(a) are well fit by this equation using an adsorption coefficient K of 2800 L/mol. The good agreement between the experimental data and Eq. (7) suggests that the use of a Langmuir adsorption isotherm and equilibrium considerations are reasonable for describing the underlying chemical process that induces drop movement for the system investigated here. We also consider the application of Eq. (7) to describe data reported by Domingues Dos Santos and Ondarchuhu for the self-propelled movement of alkane drops containing an alkyltrichlorosilane on patterned glass surfaces [10]. Figure 6(b) shows that Eq. (7) is moderately effective in fitting these data with a value for K of 95 L/mol (Table I). The greater value of K for amine adsorption (2800 L/mol) compared to that for silane adsorption (95 L/mol) is surprising given that the silane forms a more robust, covalently attached molecular film. This result, which contrasts with chemical intuition, suggests that the use of Eq. (7) to describe the data in Fig. 6(a) may be inappropriate for one or both data sets.

3. Kinetic analysis

An alternative description of reactive wetting that is based on kinetic arguments has been provided by Domingues Dos Santos and Ondarcuhu [10]. Their derivation is based on Eq. (9) proposed by Raphaël [25] for the movement of a drop on an ideal surface

$$V=\frac{\gamma_{lv}\tan\theta^*}{6l\mu}(\cos\theta_a-\cos\theta_r), \tag{9}$$

where γ_{lv} and μ are the surface tension and viscosity of the liquid, respectively, l is a logarithmic scaling factor [$\ln(x_{\max}/x_{\min})$, a ratio of macroscopic and molecular lengths], and θ^* is a dynamic contact angle given by

$$\cos\theta^*=\frac{\cos\theta_a+\cos\theta_r}{2}. \tag{10}$$

Brochard and de Gennes [14] extended this approach by incorporating a kinetic element in Eq. (9) that provided a dependence of θ_r on the coverage of the adsorbate. Specifically, they assumed that the surface coverage ϕ_s is given by

$$\gamma_{lv}\cos\theta_r=\gamma_{lv}\cos\theta_a-\gamma_1\phi_s, \tag{11}$$

where γ_1 is a constant that can be determined experimentally. Brochard and de Gennes assumed a first-order kinetic process for adsorption, thereby describing the surface coverage of the adsorbate as

$$\phi_s=1-\exp(-kct)=1-\exp\left(\frac{-kcL}{V}\right), \tag{12}$$

where k, c, t, and L are rate constant for adsorption, the adsorbate concentration, the time for adsorption (for a moving drop, its length divided by its velocity), and the length of drop, respectively. Substitution of Eqs. (11) and (12) into Eq. (9) yields

$$V=\frac{\gamma_{lv}\tan\theta^*}{6l\mu}\left[1-\exp\left(\frac{-kcL}{V}\right)\right]. \tag{13}$$

We applied Eq. (13) to the data in Fig. 6(a) and obtained a reasonable fit using values of $L=3.5$ mm, $\gamma_{lv}\tan\theta^*/6l\ \mu=1.11$ cm/s, and a rate constant k of 3500 L/mol-s. For the investigated system, the similar goodness of fits by the equilibrium [Eq. (7)] and kinetic [Eq.(13)] analyses do not allow determination of the more appropriate approach for describing the DHN/$C_{18}NH_2$/CO_2H_{surf} system.

The derivation of Eq. (13) was provided by Domingues Dos Santos and Ondarcuhu [10] who suggested its ability to describe the concentration-dependent drop velocity data

for experiments on glass using drops of octane. In their experiments, their drops contained 1,1,2,2-tetrahydroperfluorodecyltrichlorosilane $[CF_3(CF_2)_7(CH_2)_2SiCl_3]$, a compound that forms a covalently attached monolayer on glass surfaces. The derivatization proceeds with a change in wettability that is sufficient to induce self-supported drop movement. Figure 6(b) presents their experimental data [10] along with fits by Eqs. (7) and (13); Table I summarizes the parameters for these fits and suggests a faster adsorption rate for the amine than the trichlorosilane. As the latter requires chemical transformations both in solution and at the surface for reaction and the former relies on a simpler acid-base process, the relative ordering of rate constants is compatible with expectations based on chemical arguments. As for the data in Fig. 6(a), the data in Fig. 6(b) are well fitted by both equations, with little difference in the goodness of the two fits. As a result, the fits do not compel a preference for one approach over the other. However, as trichlorosilanes react irreversibly with glass surfaces [10], the use of Eq. (13) (kinetic model) to describe the data in Fig. 6(b) is likely more appropriate based on chemical arguments. In contrast, the adsorption of an *n*-alkylamine on a CO_2H surface may include desorption events, thereby preventing selection of one equation as preferred over another based on chemical arguments or a comparison of the fits to the data in Fig. 6(a) by Eqs. (7) and (13).

D. Drop length effect

In the above experiments, as the liquid surface tension defines the drop shape for a given track geometry, the drop volumes and, by association, their lengths were held fixed. We examined the ability to move drops of larger volumes on our patterned surfaces, holding the width of the CO_2H tracks and the concentration of the alkylamine constant. Figure 7(a) shows that the surface reaction provides sufficient propulsion to effect the self-propelled movement of larger drops and that increases in DHN drop size resulted in decreases in drop velocity. We rationalize the observed trend in drop velocity by suggesting that an increase in drop length increases the contact area between the drop and the substrate, thereby causing a greater drag force on the drop. The result is a decrease in drop velocity to balance the forces of propulsion and resistance on the drop [Eq. (2)]. Based on these arguments, the drop velocity would be expected to *decrease* as the drops are increased in length as observed in Fig. 7(a); however, we note that this trend is opposite to that observed by Domingues Dos Santos and Ondarcuhu in related experiments. Specifically, these authors observed that octane drops containing $CF_3(CF_2)_7(CH_2)_2SiCl_3$ on glass surface *increased* in their velocity as their length was increased [Fig. 7(b)] [10]. In both cases, the drops contain a reactive species that adsorbs onto the contacting high-energy (wettable) surface and alters the wetting properties of the surface sufficiently to produce an unbalanced surface force that induces drop movement. Given the similarity in the two processes, we were interested in the source of their opposite behaviors [Figs. 7(a) and 7(b)].

Based on the above discussion of the factors that affect drop movement, we assign the differences in Figs. 7(a) and 7(b) to whether the moving drop is operating primarily in a kinetic regime or has generated its final state structure. For example, for drops that produce adlayers at their early stages of formation, longer drops provide more contact time with the surface and allow generation of adlayers with higher surface coverage and less wettable characteristics that can induce faster drop movement. At the later stages of adlayer formation, the additional contact time provided by an increase in drop length effects little additional driving force for drop movement while the increased drop length introduces a greater resistance for movement. Given these two regimes and their expected influence by the progress of the adsorption reaction, we have replotted the data from Figs. 7(a) and 7(b) on a dimensionless reaction coordinate (Fig. 8) that

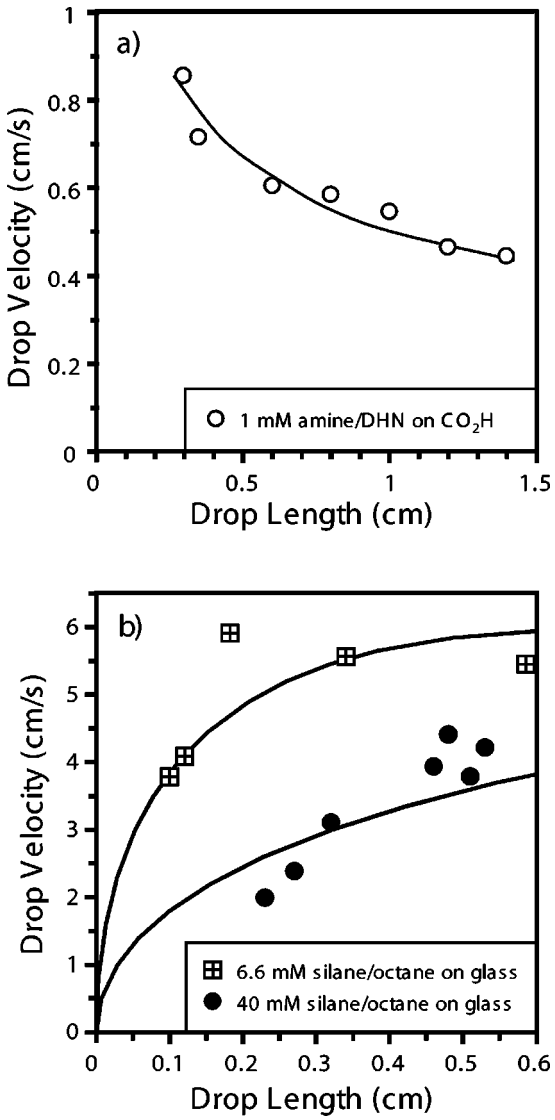

FIG. 7. Effect of drop length on the velocity of self-propelled moving drops. (a) Data for the movement of DHN drops containing 1 mM $C_{18}NH_2$ onto CO_2H surfaces. The line is provided as a guide to the eye. (b) Data taken from Ref. [10] for the movement of *n*-octane drops induced by the adsorption of $CF_3(CF_2)_7(CH_2)_2SiCl_3$ onto glass surfaces. The fits in the lower panel are to Eq. (13) where $k = 1100$ L/mole-s.

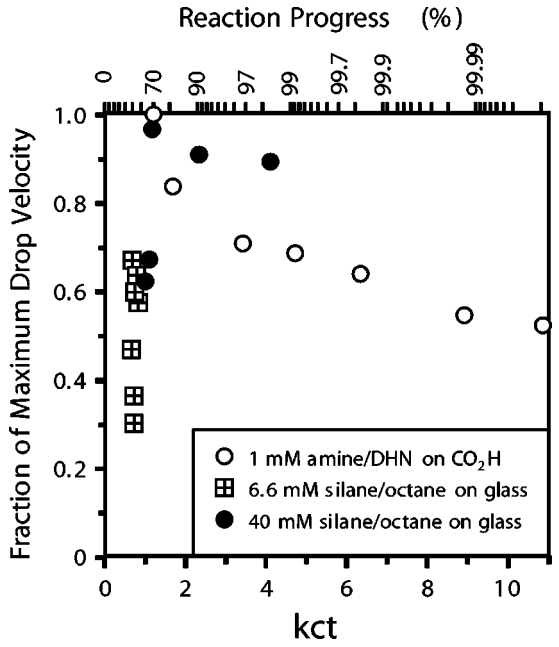

FIG. 8. Normalized velocities of moving drops for the two systems relative to a dimensionless kinetic parameter (kct) for the two different adsorption processes: $C_{18}NH_2$ onto a CO_2H surface and $CF_3(CF_2)_7(CH_2)_2SiCl_3$ onto a glass surface. Adsorption times t were calculated using drop length and velocity data ($t=L/V$), and rate constants k for the two processes were estimated from data in Fig. 6 using Eq. (7). Drop velocities for each data set were scaled to the maximum velocities predicted by Eq. (13) using the values in Table I. The top axis provides a conversion of the kct values to an extent of completion for the adlayer assuming a first-order adsorption process [$\%=1-\exp(-kct)$].

takes into account the rates of adsorption (kc) and the contact time (t) between the drop and the surface ($t=L/V$). As the two systems employ liquids with different surface tensions and produce different values of θ_r, we present the velocity data as normalized to their maximum values.

In Fig. 8, the replotted data from the two systems exhibit unifying elements. On this dimensionless axis, the data from Fig. 6(a) appear to be at late reaction times, the lower-concentration data from Fig. 6(b) appear to be at early reaction times, and the higher-concentration data from Fig. 6(b) appear to transition across the early and late reaction times. This analysis provides a framework for connecting the two reaction regimes and demonstrates the transition in drop movement behavior. The transition occurs around a surface coverage of 70% where the use of longer drops to achieve higher surface coverages and greater unbalanced surface forces are unable to compete with the simultaneously introduction of increases in drag force. The equilibrium description [Eq. (7)] appears applicable to the results presented earlier in Fig. 6(a) for $C_{18}NH_2$ adsorption onto CO_2H surfaces despite our inability to note a better fit to the data by Eqs. (7) or (13). For the data in Fig. 6(b), the kinetic analysis appears the more appropriate; however, the data point at highest concentration ($c=0.04$ mol/L and $L=0.35$ cm) may approach the limit for this analysis. Notably, the kinetic analysis by Domingues Dos Santos and Ondarcuhu to the higher-concentration data in Fig. 7(b) may not be valid as evidenced by the decrease in drop velocity upon increasing L above 0.2 cm and the correspondence of this decrease with the extent of reaction progress (Fig. 8). Notably, Fig. 7(b) captures phenomenologically the decrease in drop velocity exhibited in Fig. 8 that could not be described by the fitted model [Eq. (13)]. A complete description of the data in Fig. 8 would require suitable descriptions to correct the kinetic and thermodynamic regimes rather than approaching them separately, as done here. The evidences from this paper is that the two regimes are accessible experimentally and exhibit different phenomenological behaviors that are amenable to single chemical explanations.

IV. SUMMARY

Reactive wetting by droplets of decahydronaphthalene (DHN) containing an alkylamine can be used to direct the self-propelled drop movement on chemically patterned surfaces exposing contiguous areas of CO_2H termini surrounded by CH_3 termini. The velocity of these self-propelled drops can be effected by the chain length of the adsorbate, its concentration, and the size of drop. In general, the drop velocity increases with the adsorbate chain length and concentration, and achieves limiting values for a particular drop size. The drop velocity exhibits a decrease with the length of the DHN drop, in contrast with observations by Domingues Dos Santos and Ondarcuhu [10] for the behavior of reactive octane drops using *in situ* derivatizations by an alkyltrichlorosilane. We found that the concentration dependence of drop velocity for both data sets can be described by relationships developed based on purely thermodynamic or kinetic considerations. A difficulty is that these analyses predict sufficiently similar behaviors that are not readily distinguished by experimental results. Results examining the influence of drop length (or more appropriately drop-substrate contact time) provide a superior ability to reveal kinetic and eqilibrium regimes. Phenomenological differences between these regimes are evidenced by the observation of increasing or decreasing drop velocities for drops of increasing length. Competing factors of reaction kinetics and increased drag force yield maximum drop velocities for drop contact times that provide surface functionalization of ≈ 70–$90\,\%$ (cf. Fig. 8). For longer contact times, incremental increases in resulting surface coverages and receding wetting characteristics are offset by increases in drag force that produce a net decrease in reactively driven drop velocity.

ACKNOWLEDGMENTS

We gratefully acknowledge financial support by the Office of Naval Research.

[1] J. Simon, S. Saffer, and C.J. Kim, J. Microelectromech. Syst. **6**(3), 208 (1997).
[2] C. A. Chen, J. H. Sahu, J. H. Chun, and T. Ando, in *Science and Technology Rapid Solidification and Processing*, edited by M. Otooni (Kluwer Academic Publishers, Netherlands, 1995), pp. 123–134.
[3] F. Gao and A.A. Sonin, Proc. R. Soc. London, Ser. A **444**, 533 (1994).
[4] M. Orme, C. Huang, and T. Courter, in *Melt Spinning, Strip Casting and Slab Casting*, edited by E. Matthys and W. Truckner (The Mineral, Metals and Materials Society, Warrendale, PA, 1996).
[5] K. Schmaltz and C. H. Amon, in *Melt Spinning, Strip Casting and Slab Casting*, edited by E. Matthys and W. Truckner (The Mineral, Metals and Materials Society, Warrendale, PA, 1996).
[6] M. Vardelle, A. Vardelle, A.C. Leger, P. Fauchais, and D. Gobin, J. Thermal Spray Technol. **4**(1), 50 (1994).
[7] K. Ajito, Appl. Spectrosc. **52**(3), 339 (1998).
[8] C.-Y. Kung, M.D. Barnes, N. Lermer, W.B. Whitten, and J.M. Rarnsey, Appl. Opt. **38**(9), 1481 (1990).
[9] K.E. Miller and R.E. Synovec, Talanta **51**, 921 (2000).
[10] F. Domingues Dos Santos and T. Ondarcuhu, Phys. Rev. Lett. **75**(16), 2972 (1995).
[11] T. Ondarcuhu and M. Veyssié, Nature (London) **352**(1), 418 (1991).
[12] T. Ondarcuhu and M. Veyssié, J. Phys. II **11**(1), 75 (1991).
[13] F. Brochard, Langmuir **5**, 432 (1989).
[14] F. Brochard and P.-G. de Gennes, C. R. Acad. Sci., Ser. IIb **321**, 285 (1995).
[15] M.E.R. Shanahan and P.-G. de Gennes, C. R. Acad. Sci., Ser. IIb **324**, 261 (1997).
[16] C.D. Bain, G.D. Burnett-Hall, and R.R. Montgomerie, Nature (London) **372**, 414 (1994).
[17] M.K. Chaudhury and G.M. Whitesides, Nature (London) **256**, 1539 (1992).
[18] K. Ichimura, S.-K. Oh, and M. Nakagawa, Science **288**, 1624 (2000).
[19] S. Daniel, M.K. Chaudhury, and J.C. Chen, Science **291**, 633 (2001).
[20] S.-W. Lee and P.E. Laibinis, J. Am. Chem. Soc. **122**, 5395 (2000).
[21] Y. Xia and G.M. Whitesides, Angew. Chem. Int. Ed. Engl. **37**, 550 (1998).
[22] C.D. Bain, E.B. Troughton, Y.-T. Tao, J. Evall, G.M. Whitesides, and R.G. Nuzzo, J. Am. Chem. Soc. **111**, 321 (1989).
[23] S.-W. Lee and P. E. Laibinis (to be published).
[24] A.B.D. Cassie, Discuss. Faraday Soc. **3**, 11 (1948).
[25] E. Raphaël, C. R. Acad. Sci., Ser. IIb **306**, 751 (1988).
[26] For our investigations, the carboxylic acid surface provides a more controlled and reproducible high-energy surface than would glass which is influenced in its surface charge and adsorption characteristics by environmental factors and selected cleaning procedures.